ISSN 0140-3818
SSSU 80

# UNIVERSITY OF SOUTHAMPTON

## DEPARTMENT OF SHIP SCIENCE

## FACULTY OF ENGINEERING AND APPLIED SCIENCE

**FURTHER DEVELOPMENTS IN THE USE OF BLADE ELEMENT-MOMENTUM AND MODIFIED LIFTING LINE THEORIES TO PREDICT RUDDER-PROPELLER INTERACTIONS**

**A.F. Molland and S.R. Turnock**

**Ship Science Report 80**

**March 1994**

# FURTHER DEVELOPMENTS IN THE USE OF BLADE ELEMENT-MOMENTUM AND MODIFIED LIFTING LINE THEORIES TO PREDICT RUDDER-PROPELLER INTERACTIONS

by

A.F. Molland and S.R. Turnock

Ship Science Report No. 80

University of Southampton

March 1994

# 1. INTRODUCTION

This report describes the developments and improvements of an existing theoretical lifting line model to predict the influence of propeller loading on ship rudder performance.

Extensive experimental results of tests to determine the influence of propeller loading on ship rudder performance were reported in Refs 1 and 2. Complementary theories had been developed to provide theoretical evidence for the form of the experimental data and to allow an extension of the experimental results. These theories entailed the use of a full lifting surface approach, Ref. 3 and a simpler approach using lifting line theory, Ref. 4, the developments and improvements of which are the subject of this report.

In the lifting line analysis, lifting line theory is used to predict the spanwise load distributions. The theory is modified to include the specific features of the low aspect ratio rudder, the influence of the propeller upstream, and to account for the differences between theory and experiment.

This earlier lifting line work, described in Ref. 4, had demonstrated the feasibility of the method. Comparisons of the theoretical predictions with experimental data were very promising and indicated that the method deserved further development. Areas requiring further investigation included the characteristics of the propeller induced axial and circumferential velocities, improvements in modelling propeller slipstream contraction, the influence of non linear rudder upwash on the propeller and modifications to the modelling of the tip vortex. Applications of the method to oblique flow and low speed operation would also be investigated.

A summary of the basic theoretical analysis is given, together with descriptions of the modifications and improvements carried out. Comparisons with experimental results are given which demonstrate the suitability of the method to model rudder-propeller interaction.

## 2. GENERAL DESCRIPTION OF THE THEORETICAL MODEL

2.1 A full description of the basic structure of the theoretical model is given in Ref. 4. The following paragraphs, extracted from that reference, provide an outline summary of the theory.

2.2 The basic rudder-propeller layout is shown in Fig. 1 and the configurations investigated are shown in Fig. 2. The rudder is modelled as a lifting line with suitable spanwise input velocity and incidence distributions which result from propeller action upstream.

The propeller is modelled using blade element-momentum theory. This provides a means of estimating the induced axial and circumferential velocities at the propeller blades.

The basic propeller theory requires additional features to take account of the behaviour of the fluid between the propeller and the rudder, the influence of the adjacent hull on the propeller and the influence of the rudder on the propeller. These various features are summarised in the following sections.

2.3 The basic theory produces the induced velocities at the propeller blades. An averaging factor is required to produce the circumferential mean value at each propeller radius.

2.4 Following the behaviour of the fluid upstream of the propeller there is a further acceleration and contraction of the propeller slipstream between the propeller disc and the rudder downstream, Fig. 3(a).

2.5 Blockage effects between the propeller and adjacent hull (or wind tunnel groundboard) result in a backflow and an effective reduction in axial velocity over that adjacent part of the rudder, Fig. 3(b).

2.6 Blockage effects due to the rudder lead to a reduction in velocity over the propeller (as a whole), Fig. 3(c).

2.7 Upwash ahead of the rudder when at incidence leads to an induced crossflow in way of the propeller disc, Fig. 3(d).

## 3. PROPELLER THEORY

### 3.1 Basic Theory

The propeller induced velocities are derived using an adaptation of blade-element-momentum (BEM) theory. A summary of this theory and the equations applied are given in Ref. 4.

Axial and rotational velocity inflow factors, and hence induced axial and rotational velocities, are derived from momentum theory together with the use of Goldstein correction factors to take account of a finite number of blades.

Section thrust and torque is modelled using blade element theory in which the propeller blade is divided into a number of elemental sections. Local section lift and drag characteristics are obtained using relevant lift and drag coefficients for the particular local section type, thickness and chord length.

Combination of the momentum and blade element theories yields a solution for the induced velocities, local thrust (dT), torque (dQ) and efficiency at each elemental section. Integration of the section thrusts and torques radially across the blade yields the total thrust, torque and efficiency for each blade and hence for the propeller.

### 3.2 Further Validation of the Basic Propeller Theory

A basic assumption in the earlier analysis was that as the theoretical estimates of total $K_T$ and $K_Q$ were satisfactory, the distribution of $dK_T/dx$ and $dK_Q/dx$ would provide realistic distributions of the axial (a) and circumferential (a') inflow factors. The validity of this assumption has now been confirmed using the detailed experimental measurements of propeller induced velocities described in Ref. 5.

As before, Goldstein K factors have been applied to the downstream induced velocities (a and a') to yield the mean induced velocity and angle at each radius.

The Gutsche correction has been retained to account for the fluid acceleration between the propeller and rudder. This can be represented as:

$$K_R = 1 + 1/(1 + 0.15/(X/D))$$

and the axial and tangential velocities become:

$$V_{AR} = V(1 + K_R a)$$

$$V_{TR} = K_R a' \Omega r$$

Slipstream contraction is estimated by applying continuity between the propeller and downstream using the axial velocity changes derived by the Gutsche correction. This results in a slipstream diameter downstream ($D_R$), say at the rudder, relative to the propeller disc diameter (D) as follows:

$$D_R / D = [(1+a)/(1+K_R a)]^{1/2}$$

The results of the validation exercise are shown in Figs. 4 to 7, for the J value and X/D values used in Ref. 5.

Figure 4 shows the induced axial velocity distribution for an X/D value of 0.30. The theoretical and experimental values agree well over the outer part of the blade although the theory overestimates the velocity over the inner half. Experimental values were not available near the hub for this X/D value and it is likely that the velocity would be less than that assumed in the theory.

Fig. 5 shows the induced axial velocity distribution for an X/D value of 1.0. Here the agreement between theory and experiment is good over most of the blade. Near the hub region the theory now underestimates the velocity which has increased with increasing distance downstream of the propeller.

Figs. 6 and 7 show the induced velocity angle distributions for X/D values of 0.30 and 1.0. The theory slightly underestimates the velocity angle over much of the blade and does not predict the peak values near the blade root/hub region (r/R = 0.2). However, the overall form of spanwise distribution of velocity angle is modelled well.

It is considered that the results of the validation exercise indicate that the theory satisfactorily models the spanwise distributions of axial velocity and velocity angle. The largest errors occur in the blade root region where the axial velocities are in any case

relatively small, and their influence on the development of rudder lift will also be small.

## 3.3 Additions/Modifications to the Basic Propeller Theory

### 3.3.1 Propeller inflow velocity reduction due to rudder blockage effects

The presence of the rudder at given propeller revs causes an increase in $K_T$ which can be interpreted as an effective decrease in J (or velocity). Thus, in the theoretical model, the rudder blockage is incorporated as an effective decrease in J.

The following corrections to J are proposed in order to bring the theoretical predictions broadly in line with experimental values:

Rudder No. 2:

| J | ΔJ |
|---|---|
| 0.35 | -0.03 |
| 0.51 | -0.05 |
| 0.94 | -0.18 |

Rudder No. 3:

| J | ΔJ |
|---|---|
| 0.35 | +0.03 |
| 0.51 | 0.00 |
| 0.94 | -0.10 |

The differences due to change in rudder-propeller separation X/D were found to be very small and are not incorporated. The required corrections shown in the above tables are small, except at the very low thrust loading (J = 0.94). For Rudder No. 3, (Fig. 2) whose tip is well clear of the propeller race, different values are required with a small positive correction at high thrust loading. It is noted that this small positive correction at J=0.35 is unlikely to occur physically.

### 3.3.2 Tangential Induced Velocity at the propeller disc due to rudder upwash:

As described in Ref. 4, suitable values of upwash were obtained from the complementary lifting surface work of Ref. 3. The original theoretical model included the effect of the rudder upwash as an average (constant) value across the propeller, dependent on rudder incidence and rudder-propeller separation.

Examples of variation of the actual non-linear values of rudder induced upwash are shown in Fig. 8. These values were curve fitted and the influence on the rudder load distributions investigated.

An example of the influence of linear and non-linear distribution of upwash is shown in Fig. 9. It is noted that the effect of the inclusion of a non-linear distribution of upwash is small, as was generally the case for other thrust loadings, hence this line of investigation was not pursued.

### 3.3.3 Blockage effects between propeller and adjacent hull:

As discussed in Section 2.5, the blockage effects between the propeller and adjacent hull (or wind tunnel groundboard) result in an effective reduction in the induced velocity over the adjacent part of the rudder. The theory used in the current analysis is not capable of predicting this velocity reduction.

Empirical flow reduction factors were introduced (RED1, RED2 shown in Fig. 10) which were derived by matching the theory with the experimental data.

It was evident that due to propeller rotation this effect was not symmetrical, and separate corrections were required for positive and negative rudder incidence. The influence of propeller thrust loading (J) and rudder-propeller separation (X/D) were found to be small and did not need to be incorporated.

The derived factors are as follows:

Rudder No. 2:

| Flow Reduction Factors | Rudder Angles -30°, -20°, -10°, 0° | Rudder Angles +10°, +20°, +30° |
|---|---|---|
| RED1 | 1.00 | 1.00 |
| RED2 | 0.60 | 0.80 |

Rudder No. 3:

| Flow Reduction Factors | Rudder Angles -30°, -20°, -10°, 0° | Rudder Angles +10°, +20°, +30° |
|---|---|---|
| RED1 | 1.00 | 1.00 |
| RED2 | 0.80 | 0.80 |

It is noted that there was not a requirement to restrict the flow speed through the propeller clearance gap, i.e. RED1 = 1.0 in all cases, hence the corrections are required only over the lower half of the propeller. Also, the correction for negative incidence for Rudder No. 3, whose tip is well clear of the propeller race, is less than that required for Rudder No. 2.

## 4. RUDDER LIFTING LINE THEORY

### 4.1 General

The theory is fully described in Ref. 4 and is generally along the lines of that due to Glauert, Ref. 6, with modifications for applications to low aspect ratio ship rudders as described in Ref. 7. These modifications entail incorporating downwash contributions from the tip trailing vortex and empirical corrections to take account of the differences between theoretical lift curve slopes and those derived from experiments.

Propeller induced axial and rotational velocities are modelled as local changes in lifting line velocity:

$$V_R/V = [\pi^2 x^2 (K_R a')^2/J^2 + (1 + K_R a)^2]^{1/2}$$

and incidence:

$$\beta = \tan^{-1} \frac{\pi x}{J} \cdot \frac{K_R a'}{(1+K_R a)}$$

Hence at any point on the rudder the net incidence of the rudder, considered as a lifting line, will be:

$$\bar{\alpha} = \delta \pm \beta$$

where $\delta$ = incidence of the rudder

$\beta$ = fluid inflow angle at the rudder induced by the propeller.

The correction to the theoretical lift slope is retained as in the earlier version of the analysis and amounts to a correction to the lifting line of the form:

$$C_{Lc} = C_{Lt} \cdot e\ (AR)$$

where $C_{Lt}$ is the theoretical lift from lifting line theory

$C_{Lc}$ is the corrected lift coefficient

e is the ratio of the experimental to the theoretical and is a function of aspect ratio.

The correction proposed in Ref. 7 and adopted in the current analysis is:

$$e = 1.052\ T^{0.1}\ .\ 0.875\ (1.14AR + 2)/(AR + 3.9)$$

The influence of the tip trailing vortex was investigated further resulting in modified corrections which are described in the next section.

### 4.2 Corrections to the Tip Trailing Vortex:

It has been assumed, as described in Ref. 7, that the influence of the tip vortex is responsible for the non-linear component of lift normally exhibited by low aspect ratio lifting surfaces operating in a free stream. The assumption is also incorporated in the current analysis when the rudder is operating downstream of a propeller.

Based on the reasoning in Ref. 7 the equation used in the analysis for the downwash induced by the tip vortex is:

$$\alpha_T(\theta) = 0.645\ H_1(\theta)\ \alpha^2\ T^{1.5}/AR$$

where $H_1(\theta)$ is the general form of the variation of downwash across the span at a particular incidence, aspect ratio and taper ratio, and the constant is introduced to correlate the magnitude of the load with experiment at the datum angle. The distribution of $H_1(\theta)$ is shown in Fig. 11.

Comparison of the theoretical and experimental results for negative incidence for the earlier work indicated that the theory was over predicting the load value induced by the tip vortex in the tip region and under predicting the load from about 50% span to the tip.

Observations from the current test programme, and from the work of others such as Kracht, Ref. 8, indicate that at positive incidence the tip vortex is well defined and lifting from the rudder whilst at negative incidence the vortex is not clearly defined. This therefore results in a difference in the tip load distribution for positive and negative incidence. This difference is due to the direction of rotation of the propeller and the flow angles which it produces at the tip and this effect either increases or decreases the effective incidence of the rudder. In the current analysis, in which left-handed propeller rotation is assumed, the effective incidence is increased at positive incidence and decreased for negative incidence. This induces a greater tip vortex with positive helm and dampens it for negative helm.

A correction has been introduced to reduce $H_1(\theta)$ by the amount required to give the correct distribution at negative incidence. Since the original equation is not dependent on whether the rudder is at negative or positive incidence a statement defining this must also be introduced.

The correction to the basic assumed induced downwash distribution is incorporated as follows:

$$H_{1c}(\theta) = H_1(\theta) \cdot g \quad for\ \bar{\alpha} < 0$$

where $H_{1c}(\theta)$ is the corrected induced downwash distribution for negative rudder incidence. A suitable value for the correction factor g, derived from experimental data is as follows:

$$g = 0.679\ J + 0.1846$$

It is found that this correction is not required for the type of rudder which extends outside the propeller race, for example Rudder No. 3 used in the current investigation (Fig. 2). This limitation is incorporated in the prediction model, and the correlation of theory with experiment for Rudder No. 3, discussed later, confirms this approach.

## 5. ANALYSIS COMPUTER PROGRAM

As described in Ref. 4, the theoretical analysis, embracing the propeller theory and rudder lifting line theory has been incorporated in a computer program written in FORTRAN. This program has been updated to include the modifications and improvements described in Sections 3 and 4.

A general flow chart for the program is shown in Fig. 12. The analysis firstly derives the basic inflow factors induced by the propeller together with the necessary corrections. The corrected induced velocities and angles are then interpolated at the rudder lifting line control points for use in the lifting line analysis.

For given input values of propeller J and P/D and values of rudder aspect ratio, taper, sweep and incidence, together with X/D and D/S, the program outputs the spanwise distribution of lift together with its integration for total lift.

## 6. DISCUSSION OF THE THEORETICAL RESULTS

Examples of the results of the spanwise load predictions using the final modified version of the theory, together with the experimental results derived from the pressure measurements (Refs. 1 and 2) are given in Figs. 13 to 16.

The theoretical predictions are in good agreement with the experimental results over most of the span and for most angles of attack. The earlier problem of divergence between theory and experiment over the outer part of the rudder at higher negative rudder incidence (-20° and -30°) has now been overcome. This improvement is due in part to changes in the modelling of the tip vortex.

Following observations of physical flow, the effect of the tip vortex at negative incidence has been damped. The tip vortex is now modelled satisfactorily for both negative and positive angles of attack.

The theoretical predictions for overall lift are shown in Figs. 17 to 20. Good correlation between theory and experiment is displayed which is to be expected considering the close correlations now achieved for the spanwise distributions.

A number of improvements have been made to the original theory which have improved its robustness and accuracy. It is considered that the theory in its current form provides an acceptable level of accuracy for design purposes.

## 7. PARAMETRIC STUDIES

Parametric studies have been carried out to further validate the program and to illustrate its use.

An example of the influence of rudder-propeller separation is shown in Fig. 21 which indicates that there is a small increase in rudder normal force as separation is increased.

The influence of pitch ratio, for a given thrust loading, is shown in Fig. 22. It is noted that there is an increase in asymmetry of spanwise loading due to propeller rotation effects. The results indicate that although propeller thrust loading ($K_T/J^2$) is the controlling parameter, pitch ratio should be taken into account in more detailed investigations.

Other studies have included investigating the influence of rudder aspect ratio and changes in propeller coverage of the rudder (see Ref. 4). The examples given serve to illustrate the ability of the theory to correctly model many of the design features and to provide a useful tool for further investigations.

## 8. MODELLING OBLIQUE FLOW

A preliminary approach has been established which characterises the influence of oblique flow over the propeller-rudder combination when the vessel is in a turn. A crossflow, depending on drift angle, is applied to the propeller in a manner similar to that used to simulate the effects of rudder upwash, as described in Section 3.3.2. The early results are promising and reflect the broad trends derived experimentally and described in Ref. 9. Full simulation of the correct propeller flow straightening effects are likely to require further empirical correction to the theory.

## 9. MODELLING LOW SPEED OPERATION

Tests at low J values indicate a reasonable correlation with the experimental data, Ref. 10, although the accuracy of the propeller induced velocities is limited by the performance of the blade element theory at these low J values.

## 10. CONCLUSIONS

The theoretical model proposed and described in Ref. 4 has now been modified and updated in a systematic manner. The predictions of the spanwise distribution of normal force coefficient and total lift coefficient show close correlation with the experimental results.

The work carried out on the basic theoretical model has improved its robustness and accuracy. The method provides a very useful design tool for further investigation of changes in rudder and propeller geometry.

## ACKNOWLEDGEMENTS

The work described in this report covers part of the MOSES (Manoeuvring of Ships and Estimation Schemes) research project funded by the SERC through the marine Technology Directorate Ltd under SERC Research Grant Ref. No. GR/H28189, MTD Ref. No. SHP118.

## NOMENCLATURE

a) Propeller:

| | | |
|---|---|---|
| a | : | Axial inflow factor |
| a' | : | Circumferential inflow factor |
| a" | : | Tangential inflow factor |
| $C_D$ | : | Drag coefficient |
| $C_L$ | : | Lift coefficient |
| D | : | propeller diameter |
| $D_R$ | : | Slipstream diameter at the rudder |
| J | : | Propeller advance coefficient (V/nD) |
| K | : | Goldstein correction factor |
| $K_R$ | : | Gutsche slipstream acceleration factor |
| $K_T$ | : | Thrust coefficient ($T/\rho n^2D^4$) |
| $K_Q$ | : | Torque coefficient ($Q/\rho n^2D^5$) |
| n | : | Propeller revs/sec |
| P | : | Pitch |
| r | : | Radius of elemental section |
| R | : | Propeller radius |
| t | : | Thickness of blade element |
| T | : | Propeller thrust |
| V | : | Propeller speed of advance (or free-stream velocity) |
| $V_T$ | : | Tangential velocity at propeller induced by rudder |
| x | : | Non-dimensional coordinate (x = r/R) |
| $\alpha$ | : | Section angle of attack (relative to inflow direction) |
| $\Omega$ | : | Propeller angular velocity, rads/sec ($=2\pi n$ rps) |
| $\rho$ | : | Density of water |

**b) Rudder**

| | | |
|---|---|---|
| A | : | Total rudder area |
| AR | : | Effective aspect ratio |
| c | : | Chord |
| $C_L$ | : | Lift coefficient ($L/\frac{1}{2}\rho AV^2$) |
| $C_N$ | : | Normal Force coefficient ($N/\frac{1}{2}\rho AV^2$) |
| e | : | Lift curve slope experimental correction factor |
| g | : | Tip vortex correction factor |

$H_1(\theta)$ : General form of downwash variation induced by tip vortex

S : Rudder span

T : Taper Ratio

X : Distance of rudder from propeller (Fig. 1)

$V_R$ : Fluid flow velocity at rudder

$\bar{\alpha}$ : Effective rudder incidence ($\delta \pm \beta$)

$\beta$ : Final propeller induced flow input angle at rudder

$\delta$ : Rudder incidence

**REFERENCES**


1. Molland, A.F. and Turnock, S.R. 'Wind Tunnel Investigation of the Influence of Propeller Loading on Ship Rudder Performance'. University of Southampton, Ship Science Report No. 46, 1991.

2. Molland, A.F. and Turnock, S.R. 'Further Wind Tunnel Tests on the Influence of Propeller Loading on Ship Rudder Performance'. University of Southampton, Ship Science Report No. 52, 1992.

3. Turnock, S.R. 'Lifting Surface Method for Modelling Ship Rudders and Propellers'. University of Southampton, Ship Science Report No. 50, 1992.

4. Molland, A.F. 'The Prediction of Rudder-Propeller Interactions using Blade element-Momentum Theory and Modified Lifting Line Theory'. University of Southampton, Ship Science Report No. 54, 1992.

5. Blaurock, J. and Lammers, G. 'The Influence of Propeller Skew on the Velocity Field and Tip Vortex Shape in the Slipstream of Propellers'. SNAME Propellers '88 Symposium, 1988.

6. Glauert, H. 'The Elements of Aerofoil and Airscrew Theory'. Cambridge University Press.

7. Molland, A.F. 'A Method for Determining the Free-Stream Characteristics of Ship Skeg-Rudders'. International Shipbuilding Progress, Vol. 32, No. 270, 1985.

8. Kracht, A.M. 'Rudder in the Slipstream of a Propeller'. Proceedings of International Symposium on Ship Resistance and Powering Performance, Shanghai, April 11-14 1989.

9. Molland, A.F. and Turnock, S.R. 'Wind Tunnel Tests on the Effect of a Ship Hull on Rudder-Propeller Performance at Different Angles of Drift'. University of Southampton, Ship Science Report No. 76, 1994.

10. Molland, A.F. and Turnock, S.R. 'Wind Tunnel Tests on the Influence of Propeller Loading on Ship Rudder Performance: Four Quadrant Operation, Low and Zero Speed Operation'. University of Southampton, Ship Science Report No. 64, 1993.

wp51\afm\shiprep8

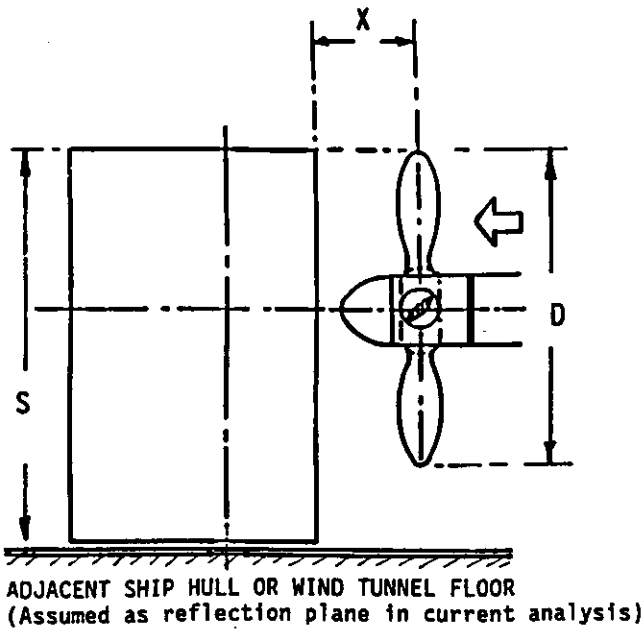


Fig. 1: Definitions of Basic Rudder - Propeller Layout

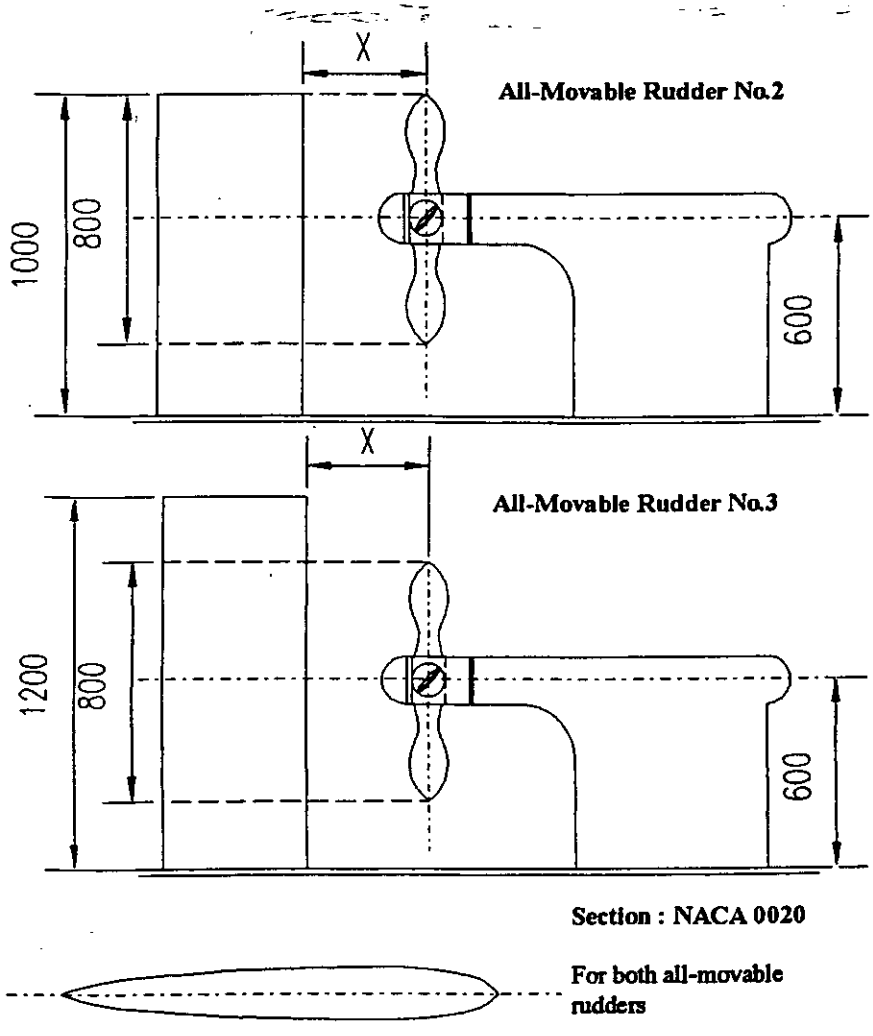


Fig. 2: Rudder-Propeller Configurations under Investigation

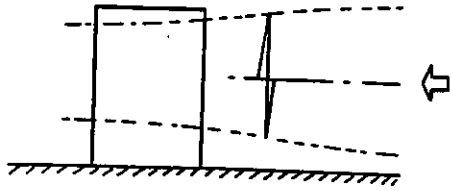

(a) Propeller Race Acceleration and Contraction

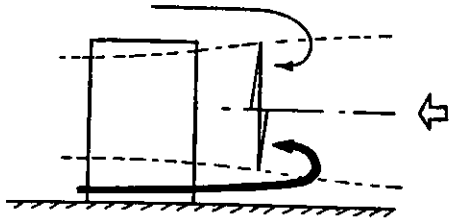

(b) Backflow Adjacent to Hull (or Tunnel Groundboard)

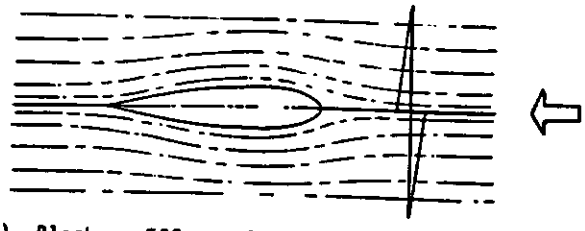

(c) Blockage Effect of Rudder on Propeller

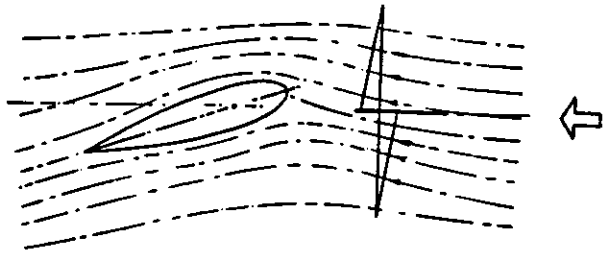

(d) Rudder Upwash leading to Crossflow at the Propeller

Fig. 3: Features of Physical Fluid Flow

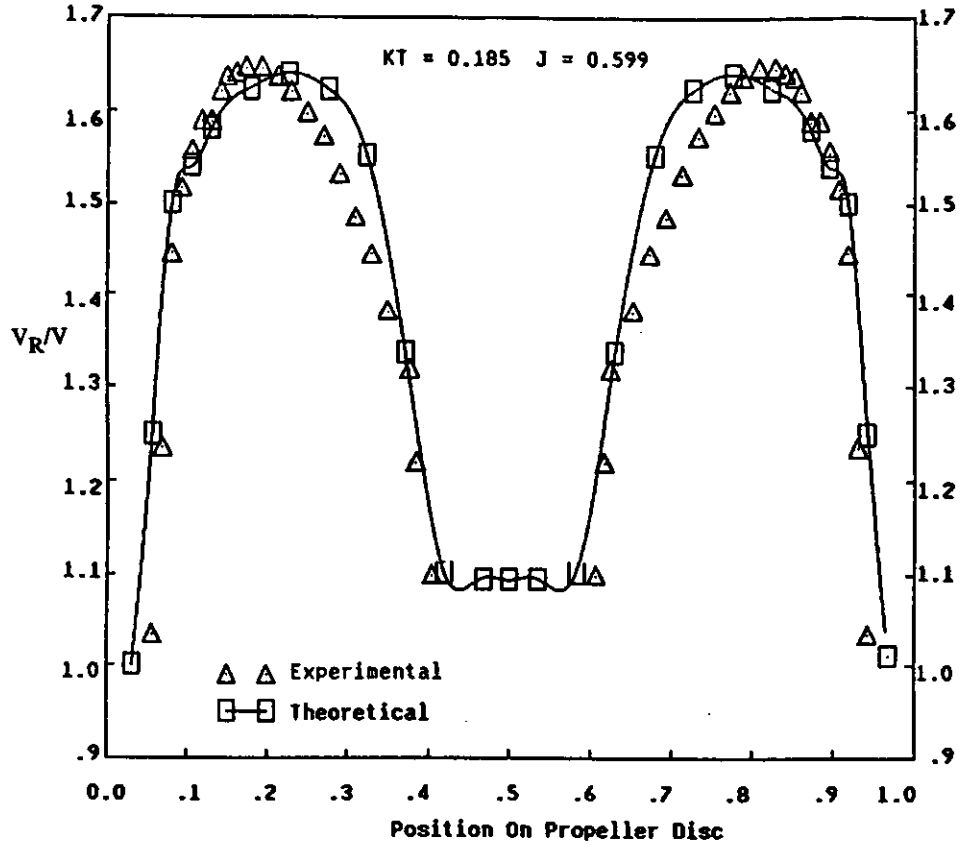


Fig. 4: Comparison of Theoretical and Experimental Propeller Axial Velocity Distributions, X/D = 0.30

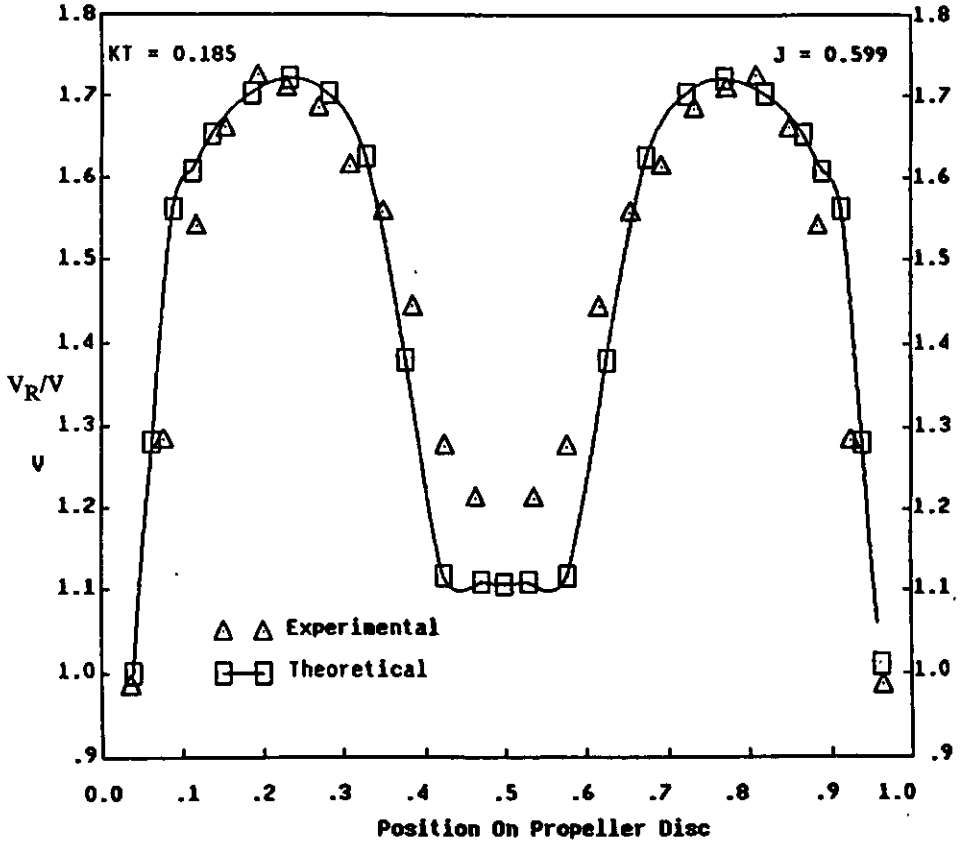


Fig. 5: Comparison of Theoretical and Experimental Propeller Axial Velocity Distributions, X/D = 1.0

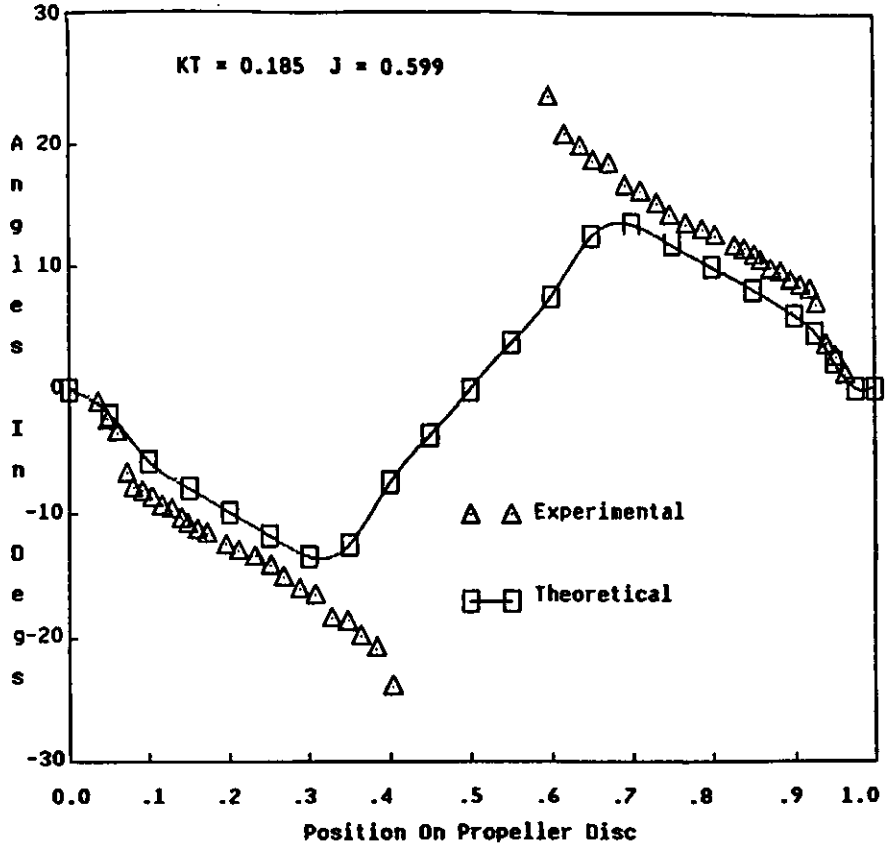


Fig. 6: Comparison of Theoretical and Experimental Propeller Velocity Angle Distributions, X/D = 0.30

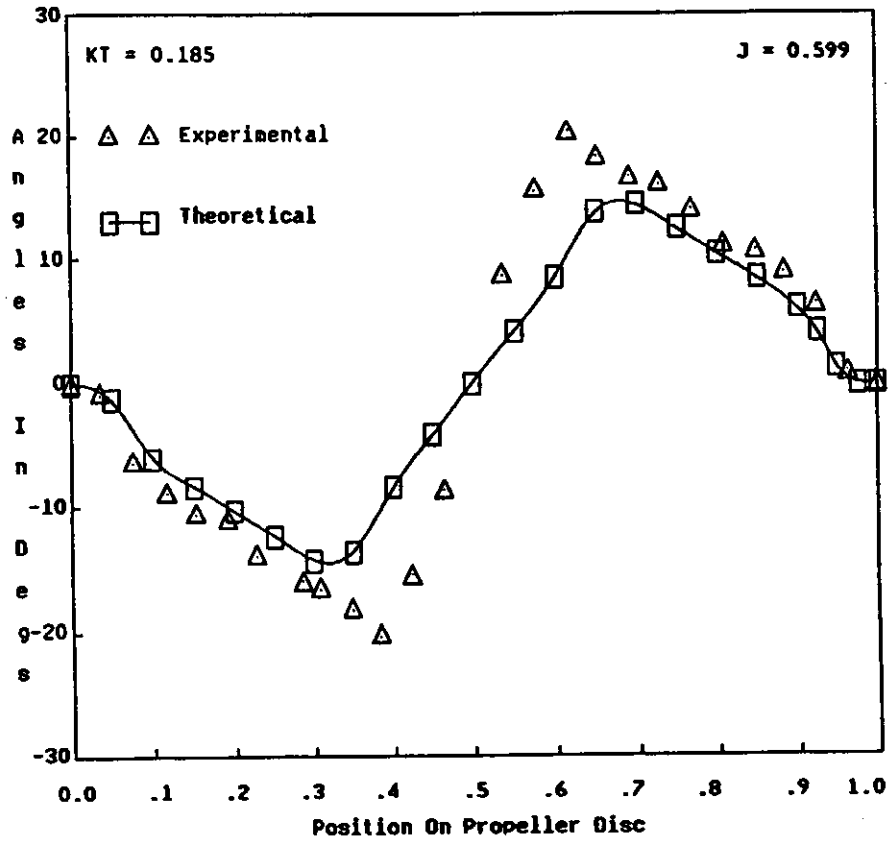


Fig. 7: Comparison of Theoretical and Experimental Propeller Velocity Angle Distributions, X/D = 1.0

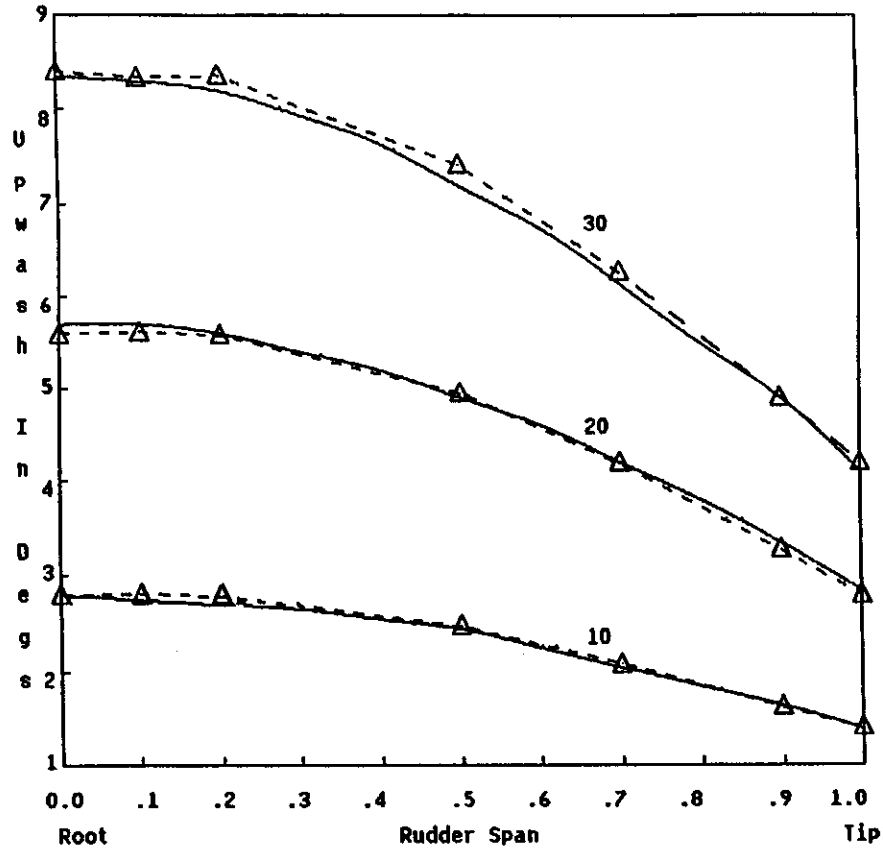


Fig. 8: Comparison of Theoretical Interpolation of Upwash Distribution over Rudder Span with Experimental Results, X/D = 0.39

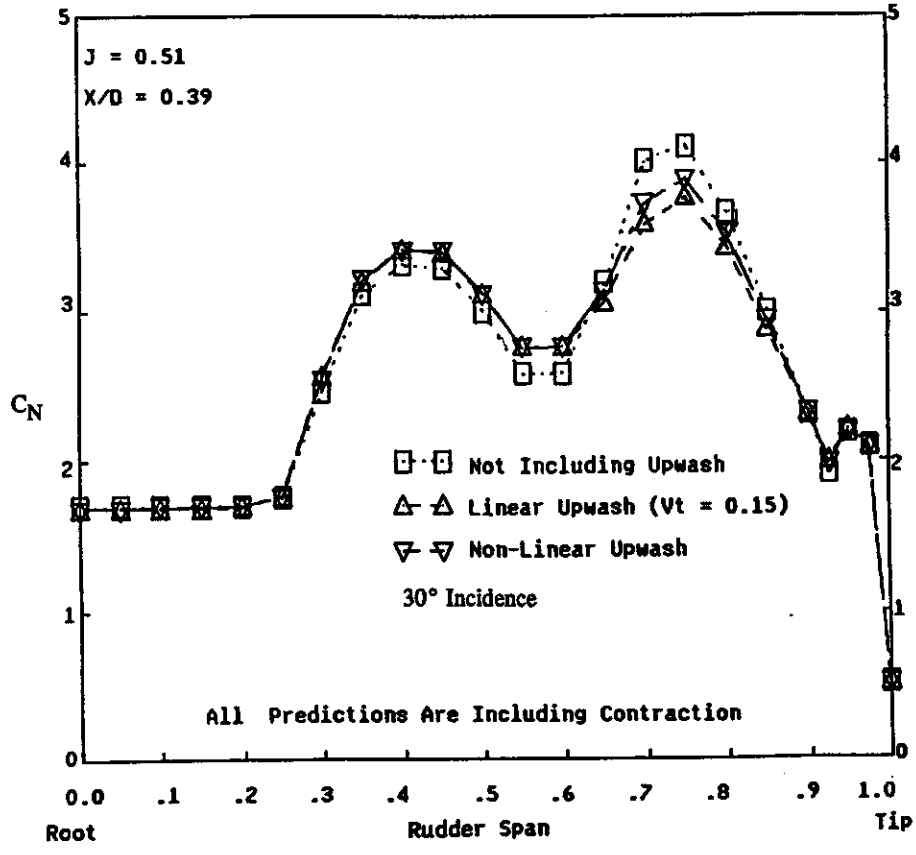


Fig. 9: Comparison of Distribution of Spanwise Normal Force Coefficient using Average and Non-Linear Distributions of Upwash

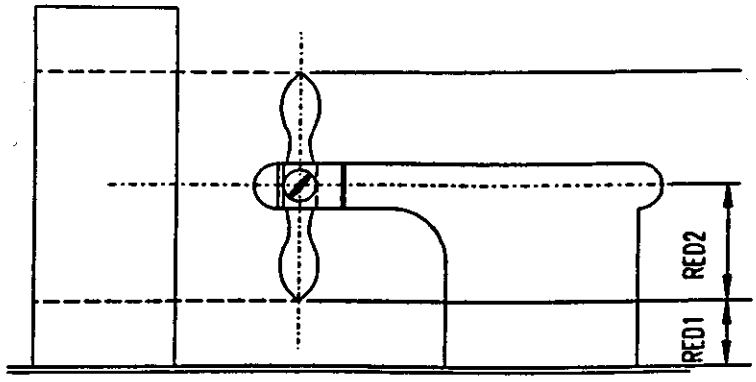


Fig. 10: Area of Application of Flow Reduction Factors, RED1 and RED2

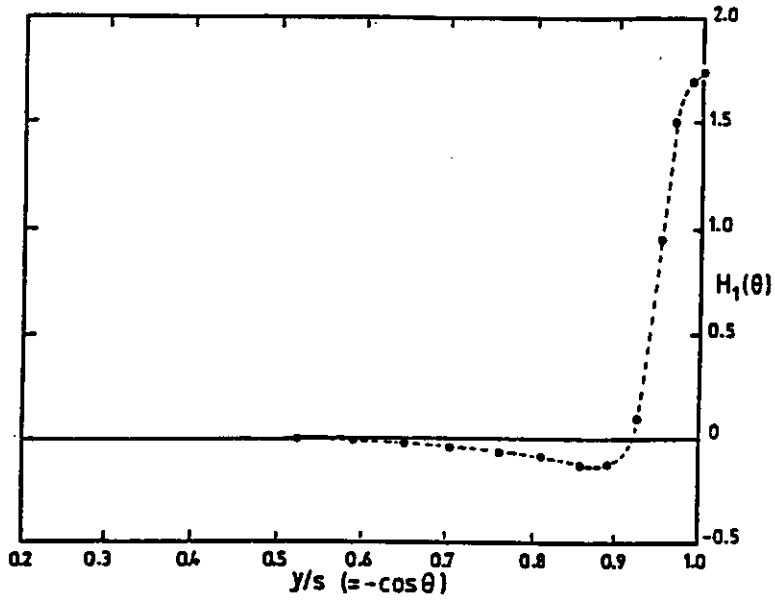


Fig. 11: General Form of Function $H_1(\theta)$

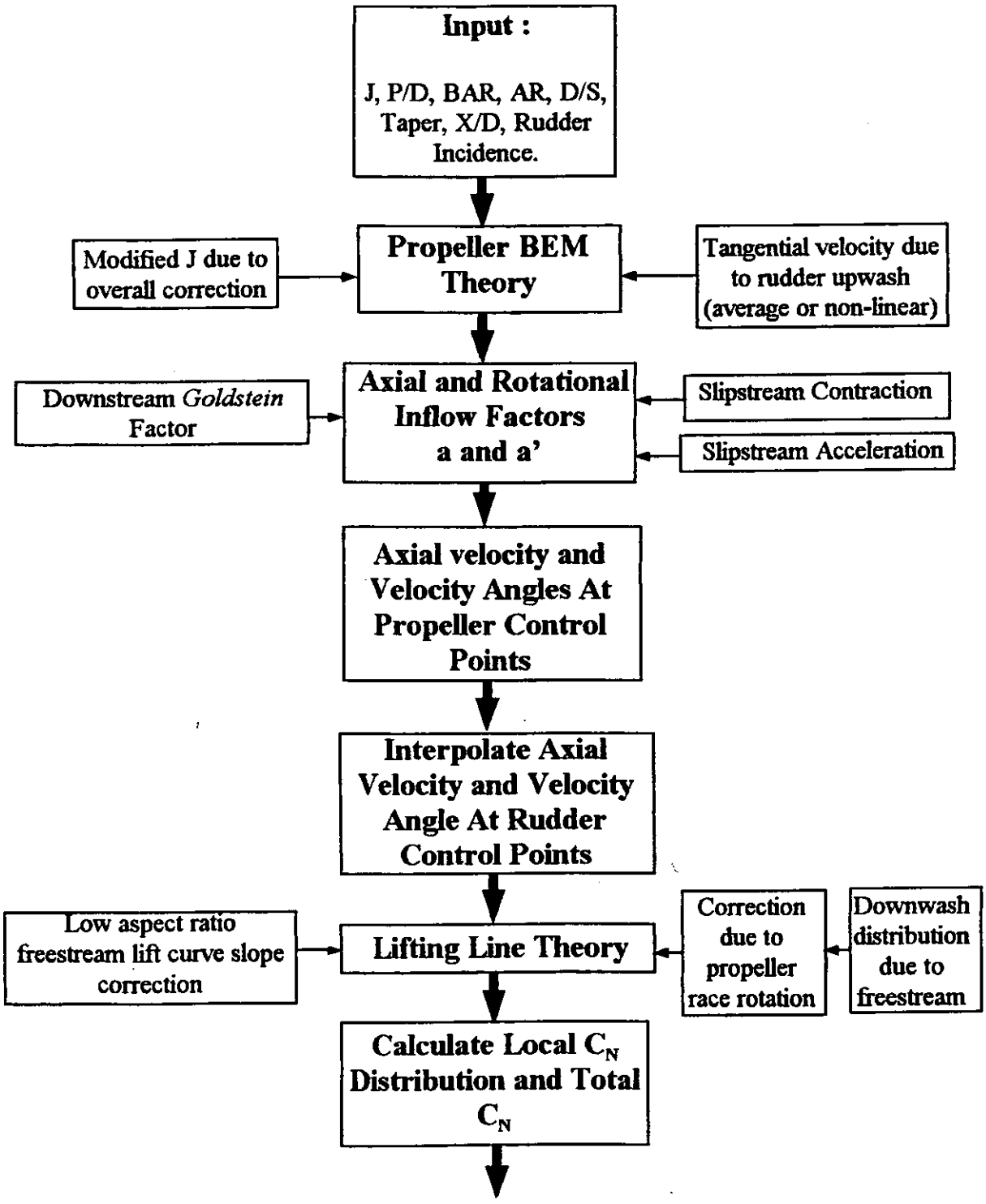


Fig. 12: Overall Computer Program Flow Path

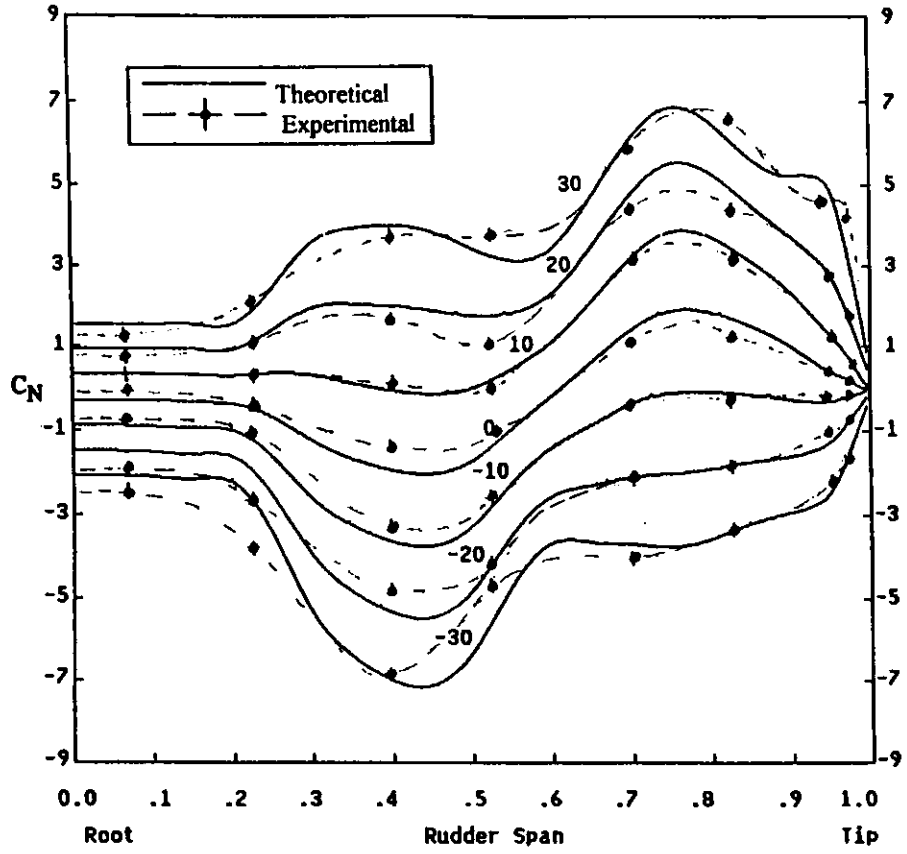


Fig. 13a: Theoretical Prediction of Spanwise Normal Force Coefficient Compared with Experimental Results

Rudder No 2, J = 0.35, X/D = 0.30

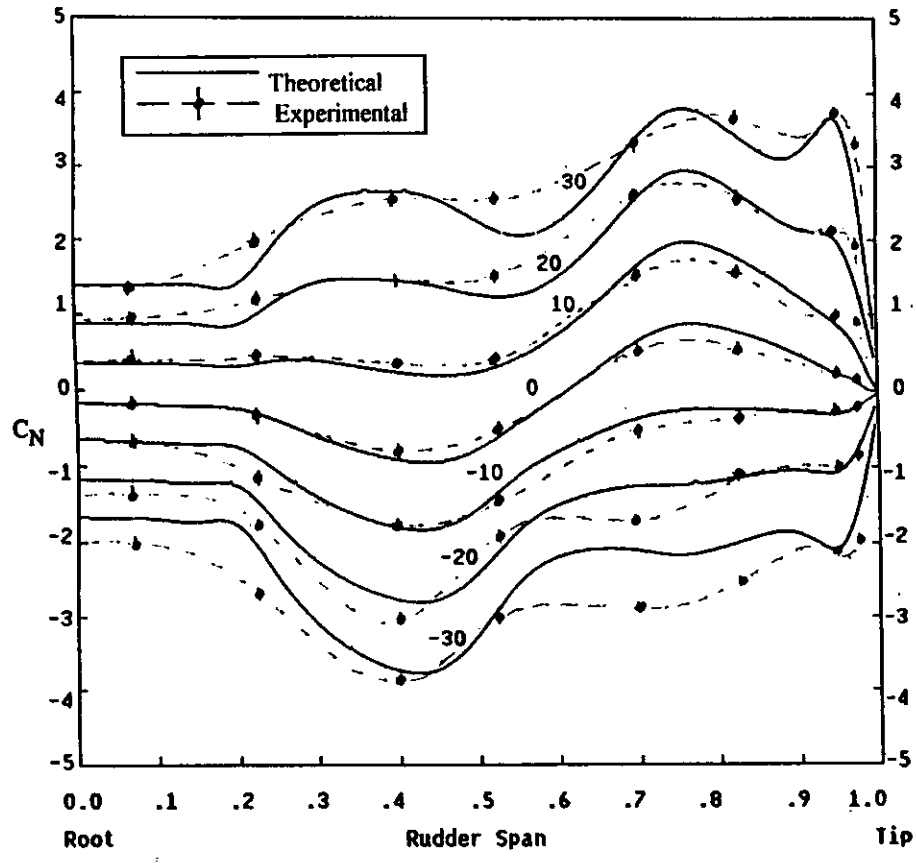


Fig. 13b: Theoretical Prediction of Spanwise Normal Force Coefficient Compared with Experimental Results

Rudder No 2, J = 0.51, X/D = 0.30

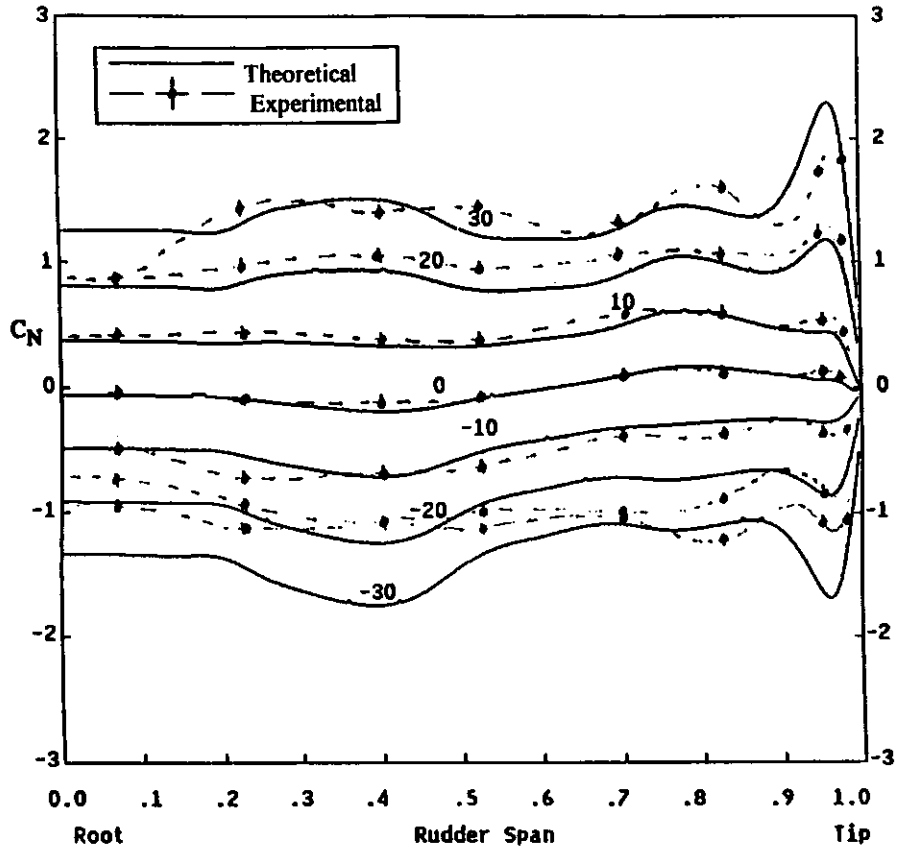


Fig. 13c: Theoretical Prediction of Spanwise Normal Force Coefficient Compared with Experimental Results
Rudder No 2, J = 0.94, X/D = 0.30

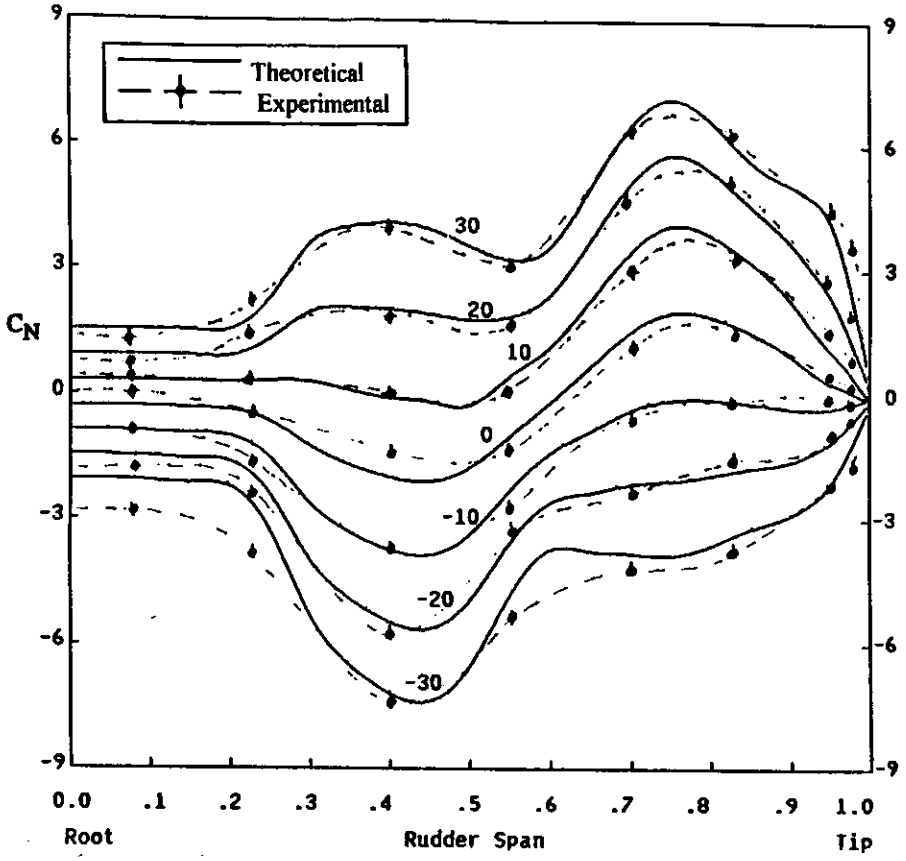


Fig. 14a: Theoretical Prediction of Spanwise Normal Force Coefficient Compared with Experimental Results

Rudder No 2, J = 0.35, X/D = 0.39

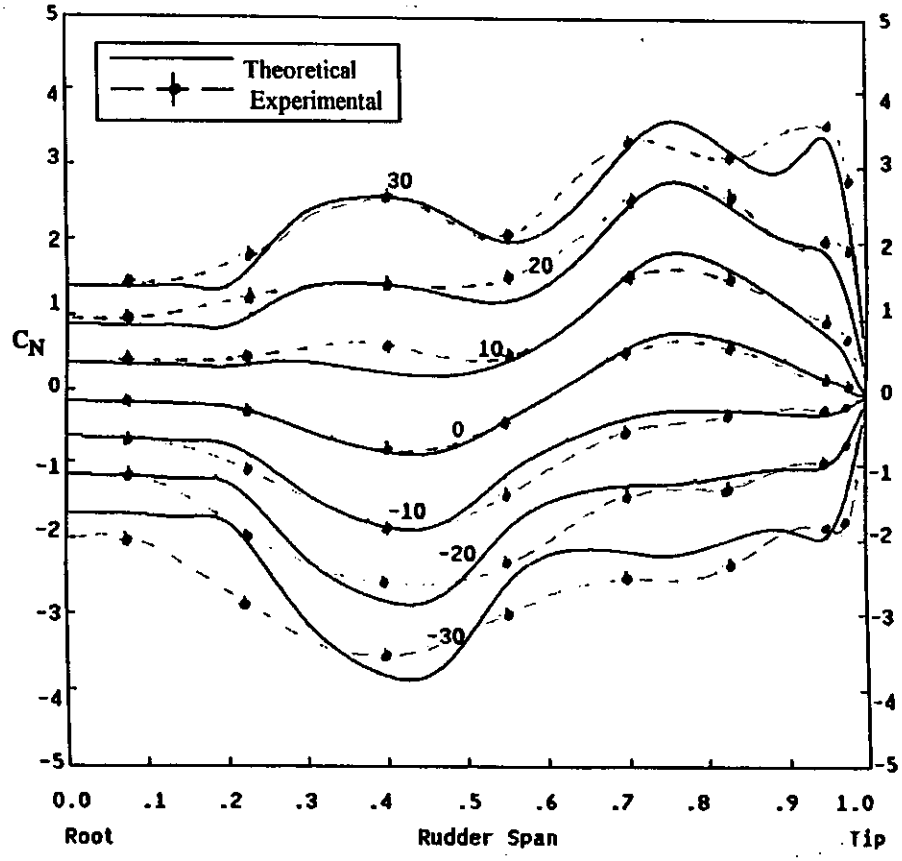


Fig. 14b: Theoretical Prediction of Spanwise Normal Force Coefficient Compared with Experimental Results

Rudder No 2, J = 0.51, X/D = 0.39

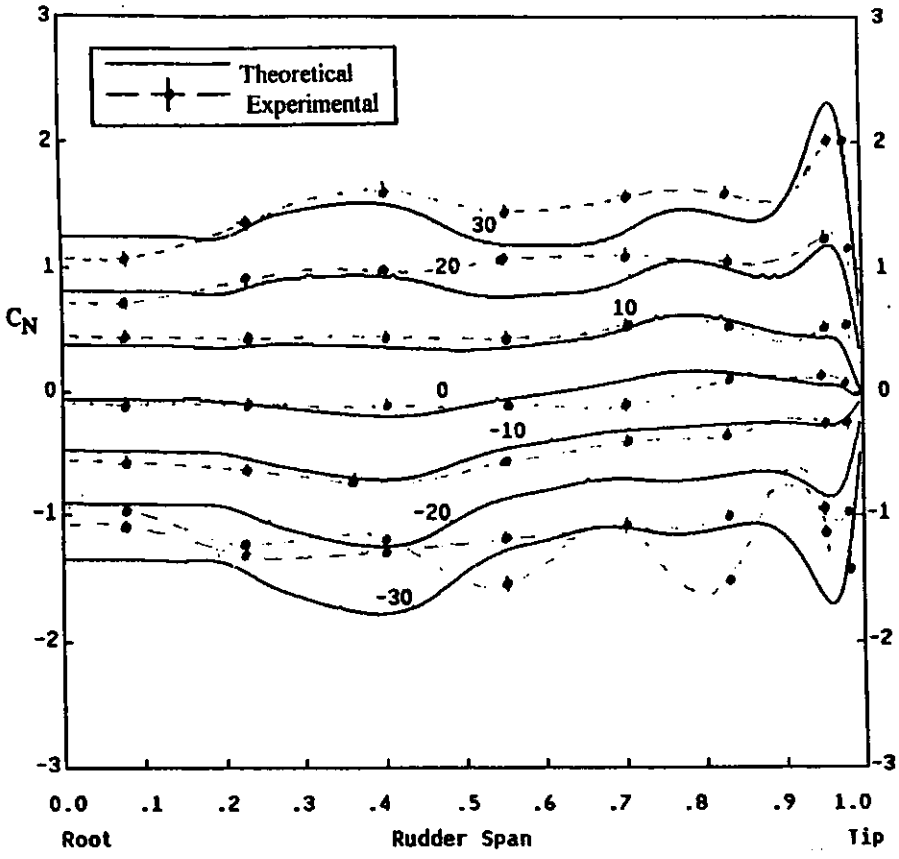


Fig. 14c: Theoretical Prediction of Spanwise Normal Force Coefficient Compared with Experimental Results

Rudder No 2, J = 0.94, X/D = 0.39

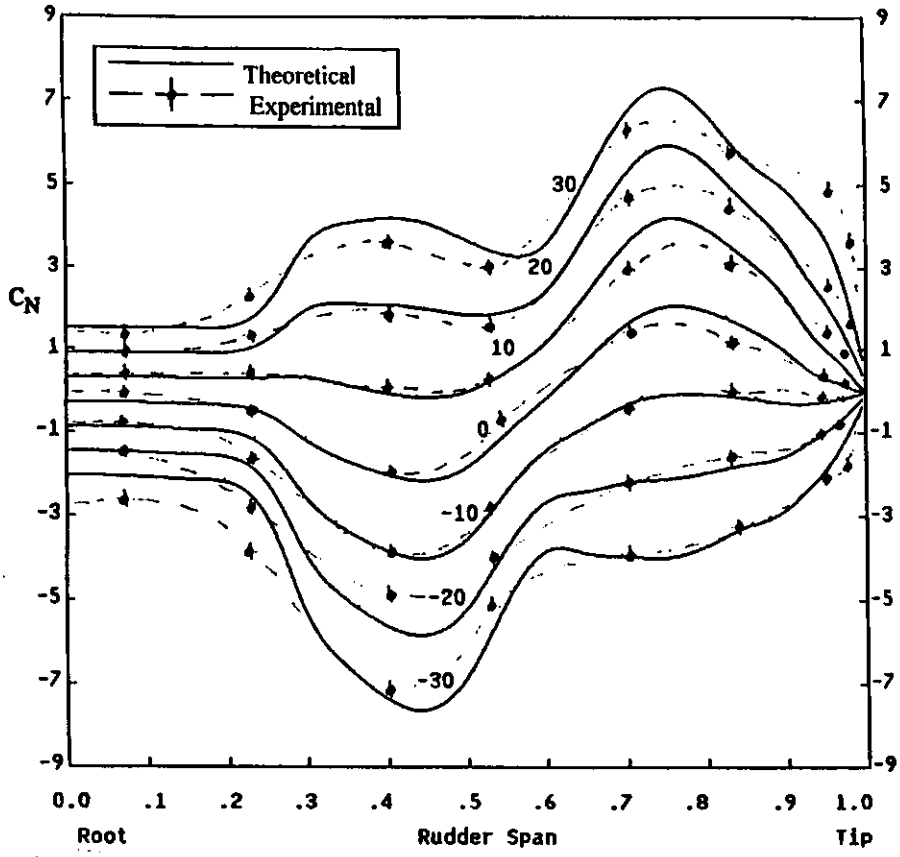


Fig. 15a: Theoretical Prediction of Spanwise Normal Force Coefficient Compared with Experimental Results

Rudder No 2, J = 0.35, X/D = 0.52

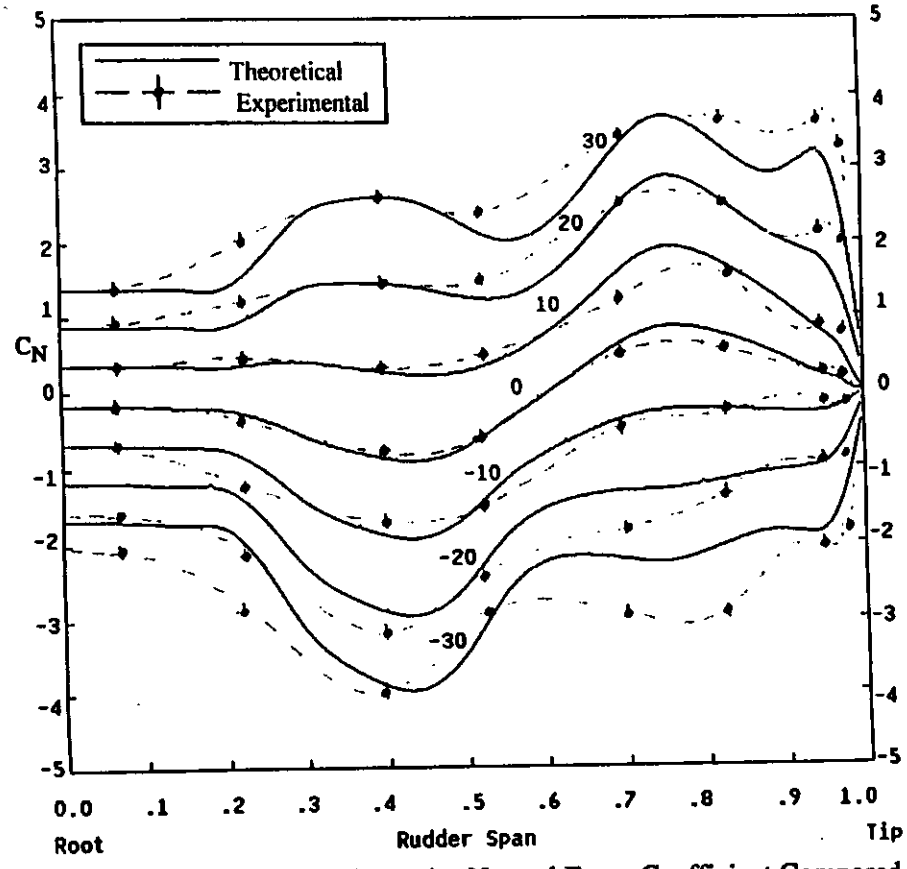


Fig. 15b: Theoretical Prediction of Spanwise Normal Force Coefficient Compared with Experimental Results

Rudder No 2, J = 0.51, X/D = 0.52

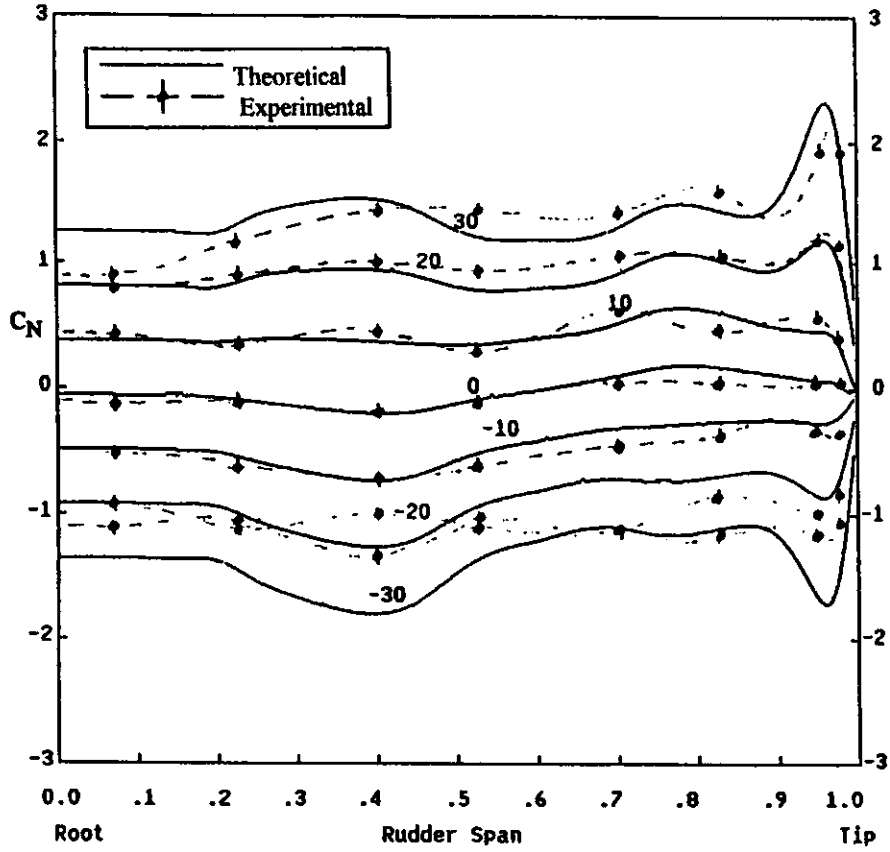


Fig. 15c: Theoretical Prediction of Spanwise Normal Force Coefficient Compared with Experimental Results

Rudder No 2, J = 0.94, X/D = 0.52

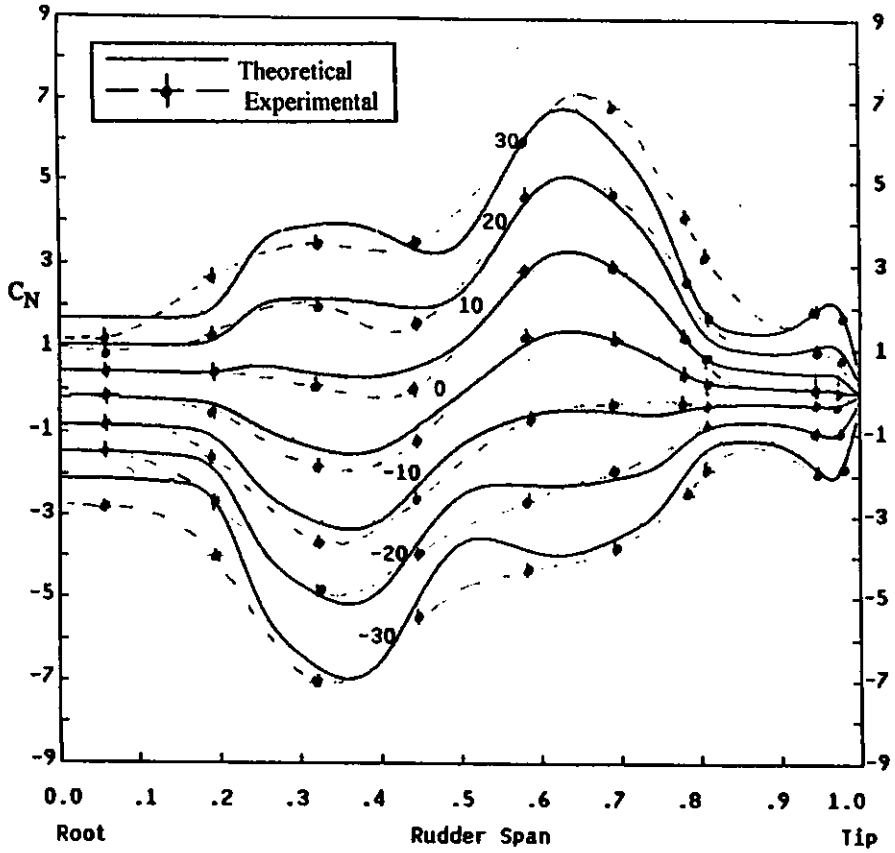


Fig. 16a: Theoretical Prediction of Spanwise Normal Force Coefficient Compared with Experimental Results

Rudder No 3, J = 0.35, X/D = 0.39

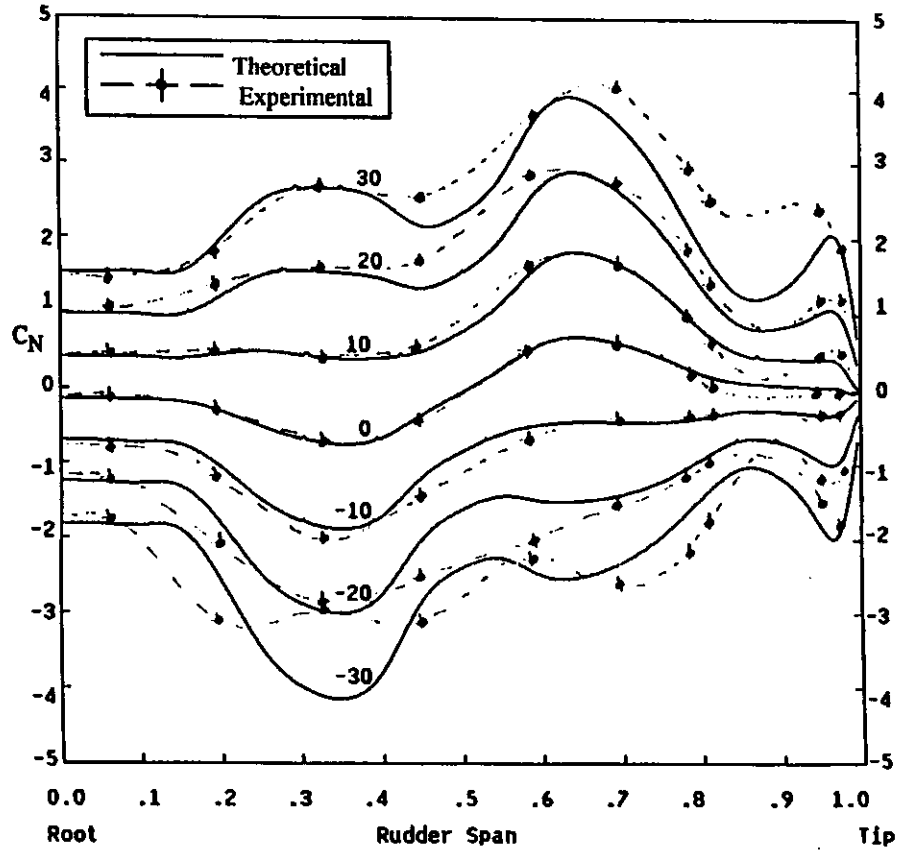


Fig. 16b: Theoretical Prediction of Spanwise Normal Force Coefficient Compared with Experimental Results

Rudder No 3, J = 0.51, X/D = 0.39

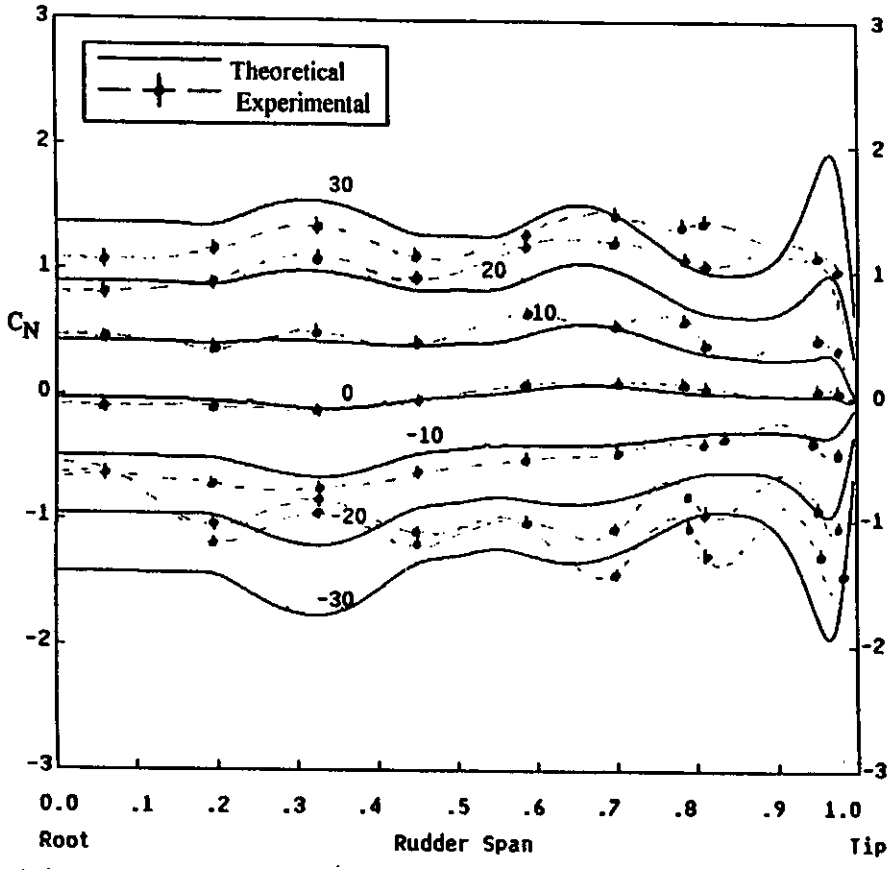


Fig. 16c: Theoretical Prediction of Spanwise Normal Force Coefficient Compared with Experimental Results

Rudder No 3, J = 0.94, X/D = 0.39

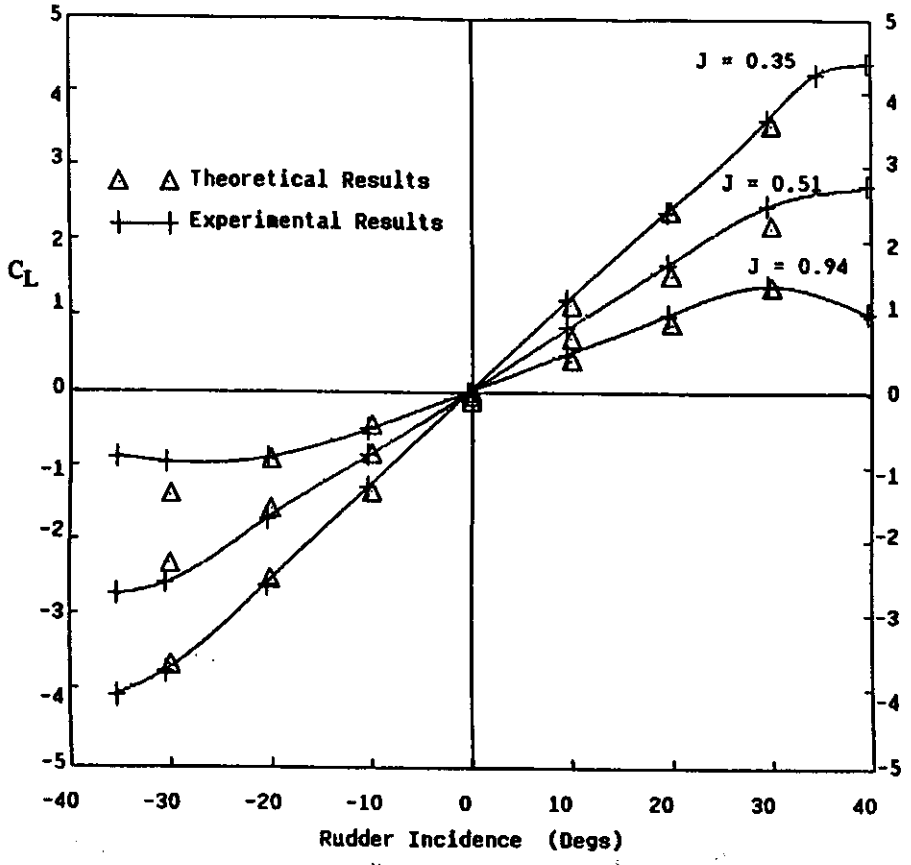


Fig. 17: Theoretical Predictions of Total Lift Coefficient Compared with Experimental Results,
Rudder No 2, X/D = 0.30

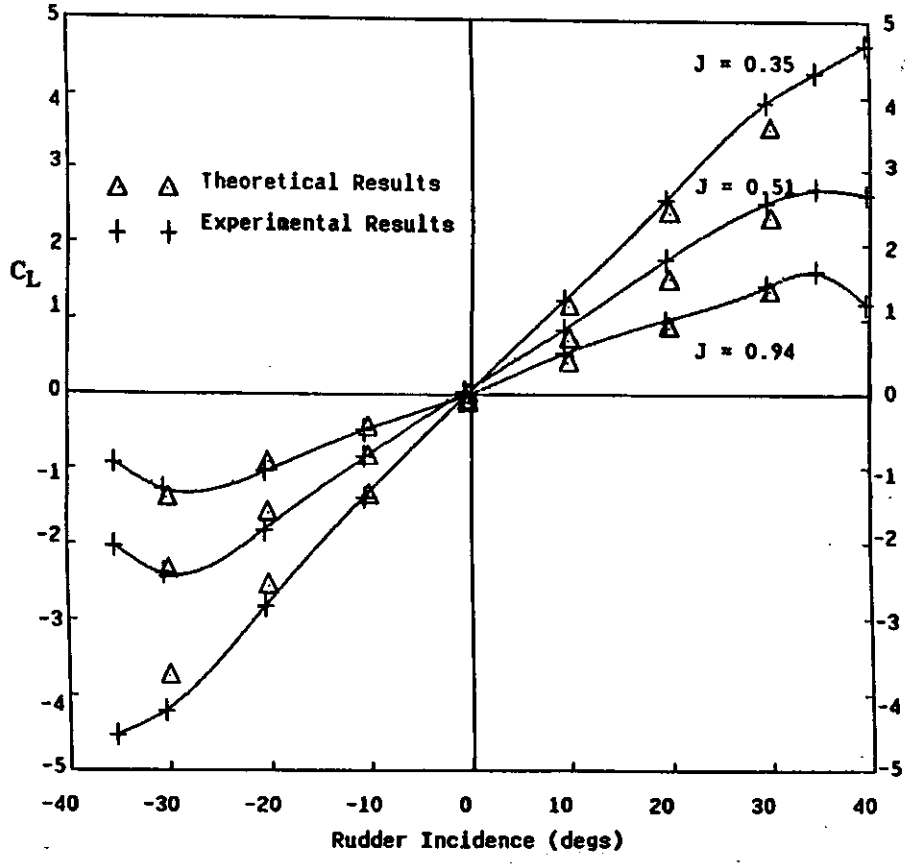


Fig. 18: Theoretical Predictions of Total Lift Coefficient Compared with Experimental Results,
Rudder No 2, X/D = 0.39

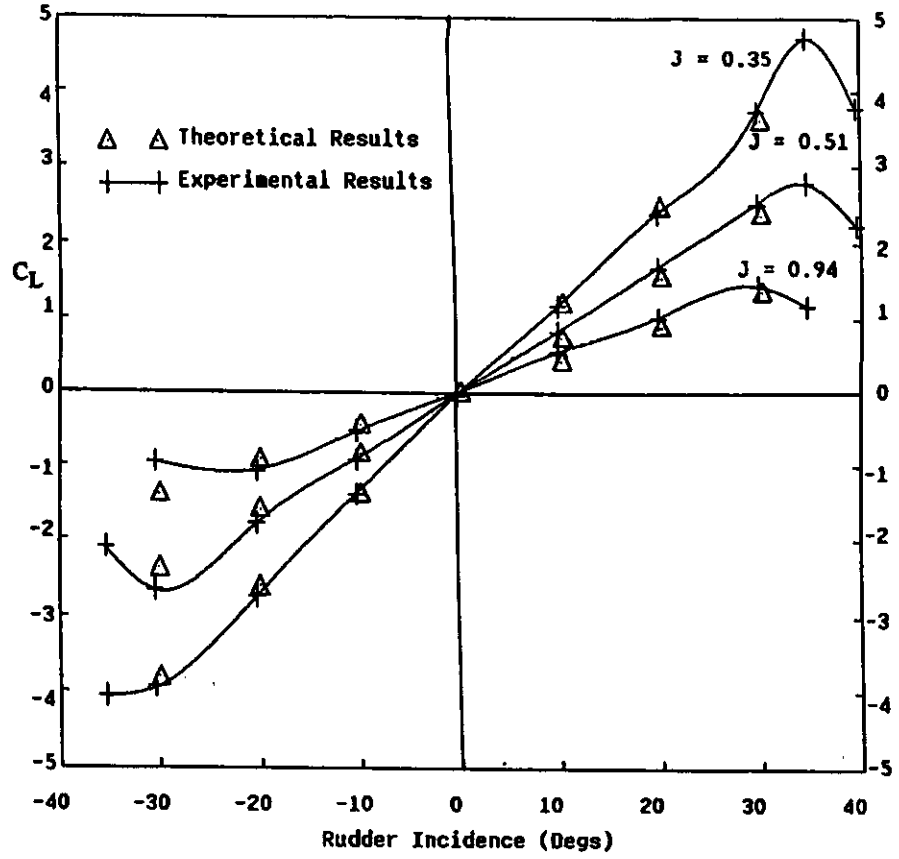


Fig. 19: Theoretical Predictions of Total Lift Coefficient Compared with Experimental Results,
Rudder No 2, X/D = 0.52

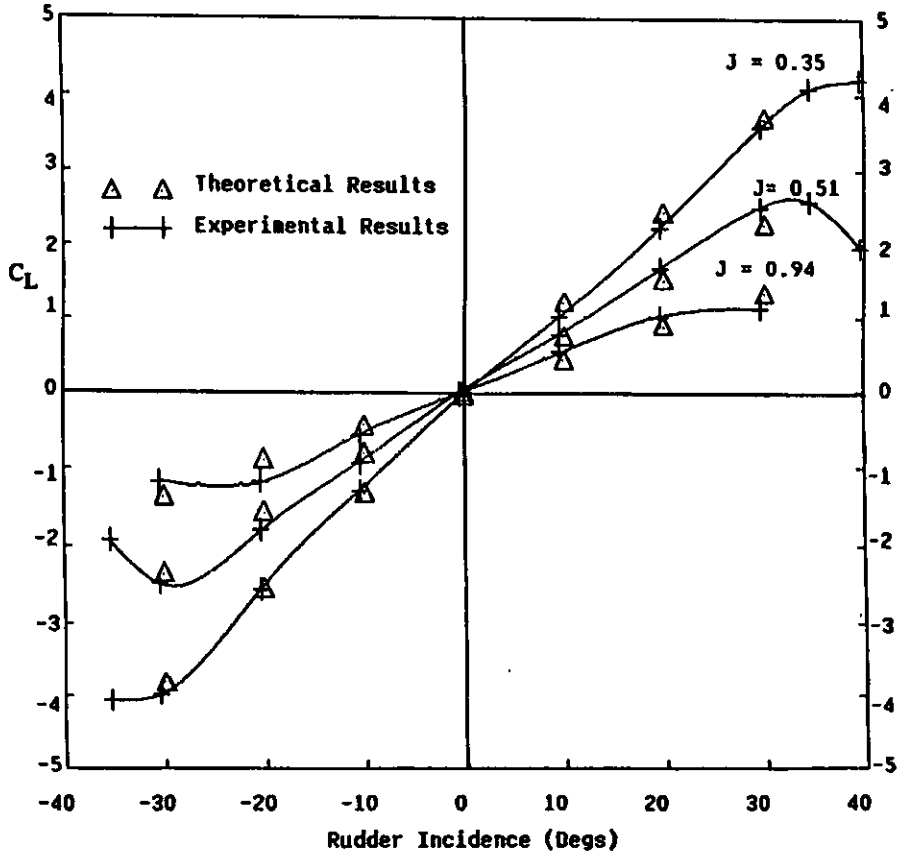


Fig. 20: Theoretical Predictions of Total Lift Coefficient Compared with Experimental Results,
Rudder No 3, X/D = 0.39

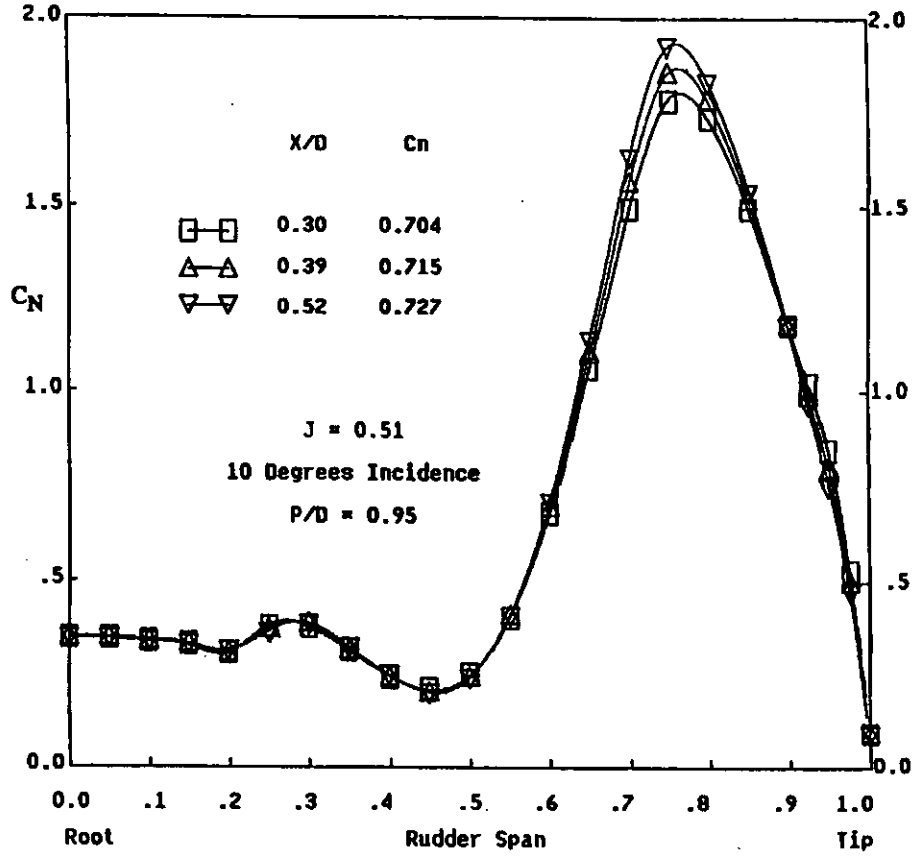


Fig. 21: Influence of Change in Rudder-Propeller Separation on Theoretical Prediction of Spanwise Normal Coefficient
Rudder No 2, 10° incidence, J = 0.51

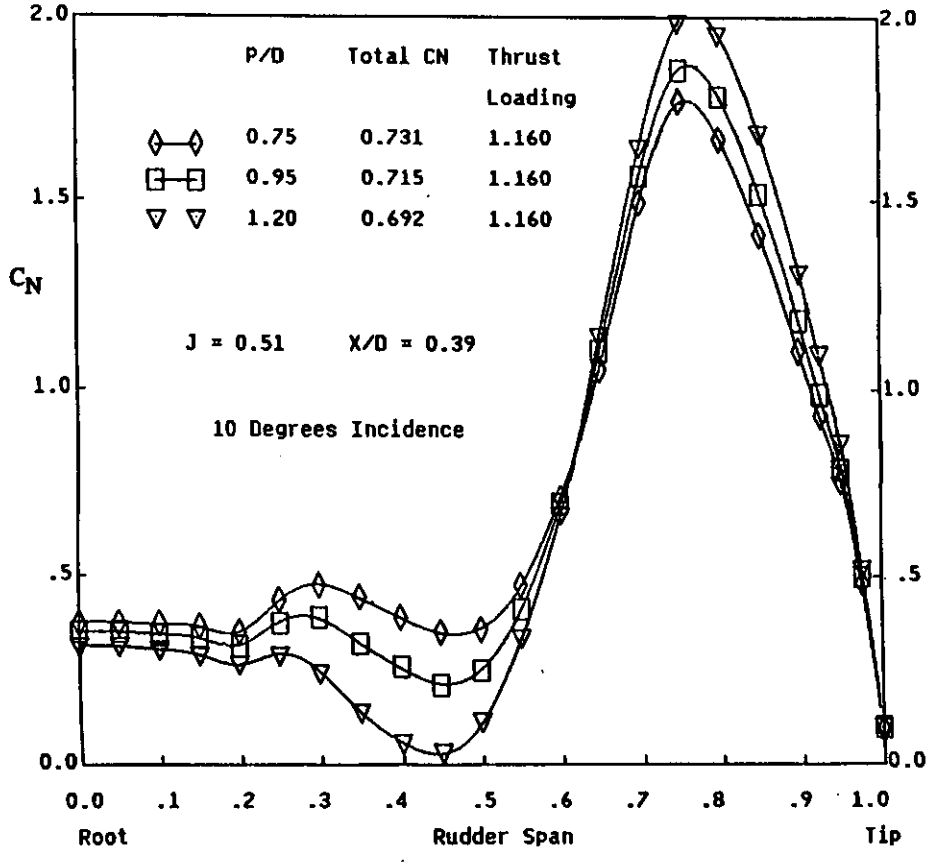


Fig. 22: Influence of Change in Propeller Pitch Ratio at Constant $K_T/J^2$ on Theoretical Prediction of Spanwise Normal Coefficient
Rudder No 2, 10° incidence, J = 0.51